PHYSICAL REVIEW B VOLUME 43, NUMBER 14 15 MAY 1991-I

Potential-barrier measurements at clustered metal-semiconductor interfaces

K. E. Miyano, David M. King, C. J. Spindt, T. Kendelewicz, R. Cao,* Zhiping Yu, I. Lindau, and W. E. Spicer
Stanford Electronics Labs, Stanford University, Stanford, California 94305
(Received 5 September 1990; revised manuscript received 20 December 1990)

Photoemission spectroscopy is commonly used to study band bending at clustered metal-semiconductor interfaces. However, these band-bending data have been difficult to interpret because of the nonuniform distribution of pinning sites. In this paper the interpretation of these measurements is investigated in detail. Using three-dimensional Poisson integration programs, we examine the extent to which the band bending can be ascribed to states at the cluster-semiconductor interfaces. First, the potential variations in the semiconductor near an individual cluster are calculated. The depletion of the semiconductor along the surface is found to be significantly less than the one-dimensional depletion length. Next, the surface-potential variations are computed for systems of known cluster morphology, assuming that the pinning states are restricted to the cluster-semiconductor interfaces. From these potentials, the expected band-bending measurements are extracted and compared to experiment. At submonolayer coverages, we find that the experimental band bending is greater than can be attributed to pinning states under the clusters. Thus, this low-coverage band bending is interpreted in terms of surface states between the clusters. Defects, chemisorbed adatoms, and surface unbuckling are discussed as possible sources of these states. Above one monolayer coverage, the clusters cover enough of the surface to uniformly pin the Fermi level. Experimentally, however, a separation between the n- and p-type surface Fermi-level positions persists to the highest coverages. This separation is also interpreted in terms of intercluster surface states.

I. INTRODUCTION

This paper concerns the interpretation of band-bending measurements based on photoelectron spectroscopy (PES). PES has been the primary technique with which Schottky-barrier formation on III-V semiconductor substrates has been measured and correlated with overlayer morphology and chemistry. One important class of overlayers is the unreactive materials, such as, In, Ga, and Ag, which cluster on room-temperature III-V substrates. Partially reactive materials such as Al and Au have also been observed to cluster on these substrates. Clustered systems have a nonuniform distribution of pinning sites on the surface, and a result, nonuniformities in the surface potential are also anticipated.[1] Such nonuniform surface potentials complicate the interpretation of band-bending measurements from these systems.

For clustered metals on III-V semiconductors, PES has detected band bending at coverages as low as 0.01 monolayers (ML).[2-4] Furthermore, for high coverages the n- and p-type surface Fermi levels are measured at separate positions in the semiconductor gap. These positions were initially attributed to donor and acceptor levels that were associated with defects induced by the deposition process.[5] The band bending at submonolayer coverages was then also interpreted in terms of the creation of such defects by the initial deposition. However, other authors[6,7] have interpreted the band bending at these clustered systems as a manifestation of metal-induced gap states[8] (MIGS) at the cluster-semiconductor interfaces. Reference 6 demonstrates that at submonolayer coverages these clusters already exhibit metallic character. In the context of the MIGS model, the high-coverage separation of the n- and p-type positions is attributed to incomplete pinning of the overall surface by these clusters.[7]

In this paper we quantitatively investigated the role of metal clusters in the overall surface-potential development. We were specifically interested in coverages for which the clusters may be treated as bulk metal.[9] At these coverages the full-coverage barrier height is established beneath the clusters, by MIGS and any other contributing mechanisms. A depletion region extends from the cluster into the semiconductor as shown in Fig. 1(a). From the cluster interface to the depletion edge, the semiconductor potential varies by the barrier height $\Delta\phi$. In particular then, potential variations on the order of $\Delta\phi$ will exist across the intercluster surface if the clusters are sufficiently separated.

Typical PES measurements have sampling depths of 15 Å or less, and so PES band-bending measurements are insensitive to the semiconductor potential beneath the clusters. Instead they derive predominantly from the varying intercluster surface potential. Our objective was to examine whether the measured potential development between the clusters could be accounted for exclusively by the interfacial charge that establishes the barrier beneath the clusters.

In the first part of this paper, the influence of an isolated cluster on the surface potential near the cluster was investigated. The extent of the lateral depletion from such

 ©1991 The American Physical Society

a cluster is quantified by the parameter $\Delta_{\parallel}$, as shown in Fig. 1(a). In a prior study[10] the one-dimensional (1D) depletion length formula

$$x_{1D} = \left[\frac{2\varepsilon_s \varepsilon_0 \Delta\phi}{qN_D} \right]^{1/2} \tag{1}$$

(where N_D is the substrate doping) was used as an estimate of $\Delta_{\parallel}$. Here the dependence of $\Delta_{\parallel}$ on the size and shape of the cluster, as well as substrate doping, was more accurately evaluated by solving the Poisson equation for the three-dimensional structure.

When $\Delta_{\parallel}$ is comparable to or smaller than the average cluster separation, the intercluster surface potential will be significantly different from the value beneath the clusters. In the second part of this paper, we explicitly calculated for such coverages the expected variation in the surface potential and the effect of such variations on PES core-level shifts and line shapes. Tang and Freeouf[1] have previously employed a two-dimensional Poisson solver to discuss in general terms the influence of a nonuniform distribution of pinning sites on the average surface potential. Here a full three-dimensional Poisson solution was applied to metal-semiconductor systems of known cluster morphology, under the assumption that the interfacial charge is restricted to that which establishes the barrier height beneath the clusters.

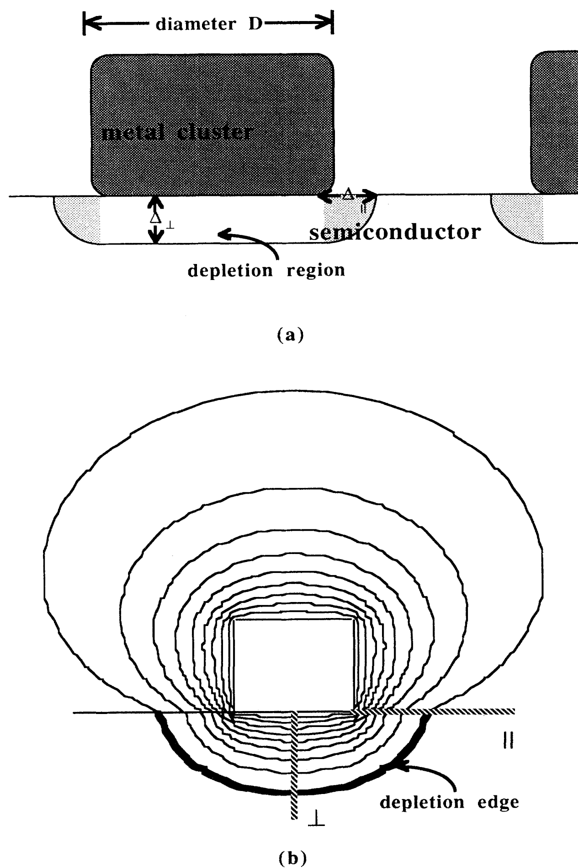

FIG. 1. (a) A metal cluster and its underlying depletion region are labeled with the parameters used in the quantitative analysis. (b) Cross section of the equipotential contour diagram generated by PISCES for a 100-Å-high by 100-Å-diam cylindrical cluster on 2×10^{18} cm^{-3} n-doped GaAs.

II. COMPUTATION

The Poisson equation was solved for metal clusters on GaAs using the finite difference method employed previously by Tang and Freeouf.[1] For isolated clusters we used the program PISCES (Ref. 11) which can solve the equation over general two-dimensional regions of metal, semiconductor, and insulator as well as three-dimensional regions with rotational symmetry about an axis. To compute the potentials for an array of clusters on a semiconductor surface, we used STRIDE,[11] a newly developed program that can handle general three-dimensional regions. In these PISCES and STRIDE calculations the surface Fermi level position at the metal-semiconductor interfaces was fixed at GaAs midgap, 0.7 eV above the valence-band maximum. This pinning can represent any mechanism that maintains a constant surface potential at the cluster, whether it be MIGS, Schottky-type band alignment, or defects isolated beneath the clusters. The same pinning position is used for n- and p-type substrates: even when defects control the pinning position, such an agreement between n- and p-type substrates is predicted for a substrate covered by a fully metallic overlayer.[12] For isolated clusters the PISCES computation is more efficient than that of STRIDE because it takes advantage of the axial symmetry, but we verified that STRIDE provides the same results as PISCES for these isolated clusters.

III. SURFACE-POTENTIAL VARIATIONS NEAR A SINGLE CLUSTER

We were interested in the extent of a metal cluster's influence on the nearby semiconductor surface potential, as represented by $\Delta_{\parallel}$ in Fig. 1(a). PISCES was used to calculate the dependence of this parameter on cluster size and shape as well as substrate doping.[13] Displayed in Fig. 1(b) is an equipotential contour map generated by PISCES for an isolated cylindrical cluster. Highlighted in this figure is the contour for which the potential variation from the interface to the bulk is 90% complete: this contour is defined as the edge of the depletion region in the present study. Depletion lengths were calculated for various cluster diameters and shapes, and we found that these lengths are insensitive to aspects of cluster shape other than the diameter. For example, cylindrical clusters with a 100 Å diam may be varied in height from 200 to 25 Å with less than a 1% variation in $\Delta_{\parallel}$. And $\Delta_{\parallel}$ for a cylindrical cluster of 50 Å height and a 100 Å diam is within 1% of $\Delta_{\parallel}$ for a hemispherical cluster with a 100 Å diam.

In Fig. 2(a), calculated $\Delta_{\parallel}$ are plotted as a function of cluster diameter D for cylindrical clusters on n-type GaAs. Also plotted for comparison is $\Delta_{\perp}$, the depletion

length below the center of the cluster [see Fig. 1(a)]. The calculations were carried out on clusters with height equal to diameter, but as mentioned above, the Δ are insensitive to the cluster height. For D as small as 25 Å, the clusters contain hundreds of atoms, and the assumption that the clusters are metal is justified. $\Delta_{\parallel}$ is always shorter than $\Delta_{\perp}$; the depletion region is in general observed to be most narrow along the semiconductor surface. In Fig. 2(b) the potential variation near the cluster of Fig. 1(b) is graphed along two directions: parallel [along the line marked $\parallel$ in Fig. 1(b)] and perpendicular (along $\perp$) to the surface. The initial potential variation from the metal cluster is stronger parallel to the surface than perpendicular, and this can be observed in the equipotential diagram of Fig. 1(b) as well. There is a strong pinching of the contours near the corners of the cluster at the cluster-semiconductor interface. So from these three-dimensional calculations we conclude that the range of influence of a cluster on the semiconductor potential is shortest along the surface. Of course, it is only along the surface that this influence can be measured with surface sensitive techniques.

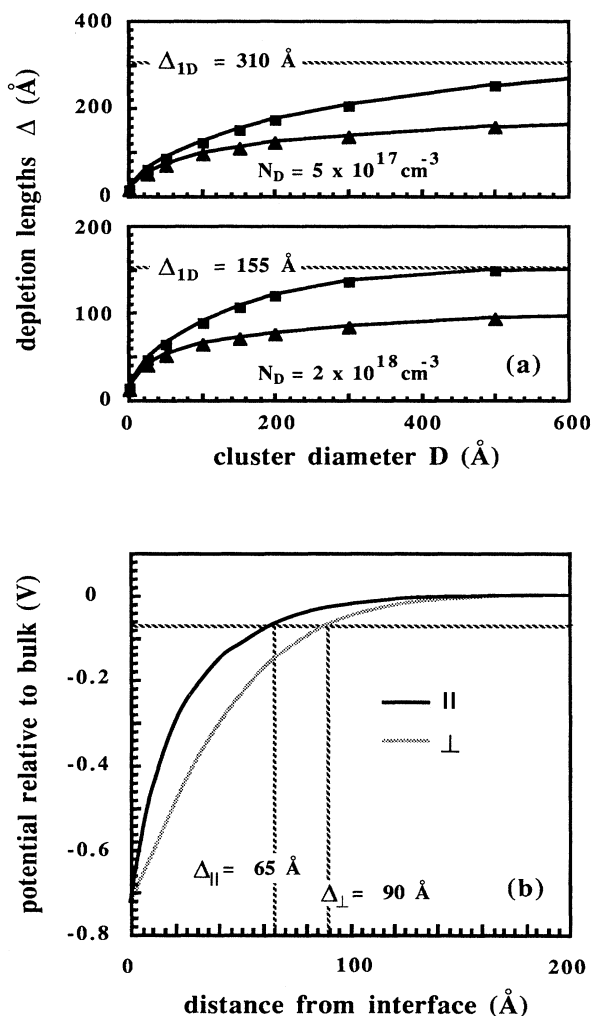

FIG. 2. (a) $\Delta_{\parallel}$ (triangles) and $\Delta_{\perp}$ (squares) are graphed vs the cluster diameter for cylindrical clusters on 5×10^{17} and 2×10^{18} cm^{-3} n-doped GaAs. (b) The potential variation along the paths $\parallel$ and $\perp$ of Fig. 1(b) is plotted with marks for the depletion lengths along these directions.

Figure 2(a) shows that $\Delta_{\parallel}$ and $\Delta_{\perp}$ are constant for large cluster diameters. For large diameters the depletion side lobes [shaded in Fig. 1(a)] constitute a small fraction of the total depletion region, and a one-dimensional analysis becomes appropriate to determine $\Delta_{\perp}$. Thus in this limit, $\Delta_{\perp}$ approaches Δ_{1D}, the depletion length determined by PISCES for a continuous overlayer on the GaAs substrates.[14] And over the doping range studied (4×10^{16} to $1\times10^{19} cm^{-3}$), $\Delta_{\parallel}$ saturates at $0.6\Delta_{1D}$. However, as the cluster diameter is reduced below about Δ_{1D}, a significant fraction of the interfacial charge is now cancelled by depletion charge in the side lobes, and the depletion region shrinks in all directions.

Thus PISCES determines that the lateral extent of the potential variation from a cluster on a semiconductor is in general smaller than any one-dimensional estimate can indicate. Even for large diameter clusters, the lateral extent of the depletion region is 40% less than the one-dimensional depletion length. Specifically, the large-cluster values of $\Delta_{\parallel}$ may be read from Fig. 2(a) to be 180 and 90 Å for the 5×10^{17} and 2×10^{18} cm^{-3} dopings, respectively. For smaller cluster sizes $\Delta_{\parallel}$ falls substantially below these levels. In the large cluster limit the depletion lengths $\Delta_{\parallel}$ and $\Delta_{\perp}$ exhibit an $N_D^{-1/2}$ dependence on the doping as given in the simple one-dimensional formula (1). For smaller diameters this simple dependence is lost, but the depletion lengths are always smaller for higher doped substrates. For a 2×10^{18} cm^{-3} doping $\Delta_{\parallel}$ is less than 100 Å for all cluster sizes. Heavily doped substrates will come into frequent usage in PES studies with the recent recognition of photovoltaic effects in lower doped samples,[15–17] and for such substrates, consideration of lateral potential variations in clustered systems will be particularly important. Next we explicitly calculated the lateral potential variations for such systems.

IV. SURFACE-POTENTIAL VARIATIONS FOR CLUSTERED SYSTEMS: INFLUENCE ON PES SPECTRA

To calculate the surface-potential variations for real metal-semiconductor systems, experimental measurements of clusters sizes and separations are needed. An earlier estimate of such parameters for coverages of In, Ga, and Ag on GaAs(110) was based on PES intensity attenuation data.[18] However, the ratio of cluster height to diameter (the aspect ratio) cannot be determined from core-level attenuations. In Ref. 18 this ratio was assumed to be one: aspect ratios of greater than one are unphysical, so this assumption provides a *lower* limit on the actual cluster separations.[19] In fact direct images of clusters on GaAs indicate that aspect ratios are closer to 0.5. Some of these images come from the reflection high-energy electron diffraction (RHEED) and scanning electron microscopy (SEM) work of Savage and Lagally[20] for the In/GaAs(110) system. The parameters of interest from their study are collected in Table I. All coverages

TABLE I. Relevant parameters from Ref. 20.

Coverage (ML)	Cluster height (Å)	Cluster size (Å)	Cluster separation (Å)
0.6	22	50	135
2	30	50	70
4	32	50	30
8	50	60	20

quoted here are effective coverages, the thickness the overlayer would have if it were uniformly covering the substrate. The cluster diameters are close to 50 Å for all four coverages, and from Fig. 2(a), it is observed that the lateral depletion length for this size cluster on a 2×10^{18} cm^{-3} n-doped substrate is around 50 Å. Referring back now to Table I, this depletion length is seen to be less than the average cluster separations for the 0.6- and 2-ML In coverages. Thus for these coverages on a 2×10^{18} cm^{-3} doped substrate, distinct lateral potential variations are expected, whereas the intercluster surface potential is anticipated to reflect the barrier height beneath the clusters for the 4- and 8-ML coverages.

Each cluster geometry described in Table I was modeled with STRIDE as a periodic array of clusters as shown in Fig. 3(a).[21] The discrepancies introduced by modeling the interfaces as a regular array of identical clusters are discussed below. In Fig. 3(b), we show the surface potential calculated for the clusters in Fig. 3(a) on 1×10^{19} cm^{-3} p-type GaAs.

We wished to determine how such potential variations would manifest themselves in a surface sensitive PES spectrum, $X(E)$, taken from the clustered interface. $X(E)$ may be constructed from $X_0(E)$, a spectrum taken at the clean, unpinned surface:[22]

$$X(E)\propto \int dx \int dy \int dz \exp(-z/\lambda)X_0(E+V(x,y,z)) \ , \tag{2}$$

where $V(x,y,z)$ is the semiconductor potential with respect to deep in the bulk, and λ is the escape depth of the photoelectrons. This integral was computed from the STRIDE potentials, $V(x,y,z)$, by adding together the spectra $X_0(E+V(x,y,z))$ over an evenly spaced grid of coordinates (x,y,z) with a weighting of $\exp(-z/\lambda)$. At the coverages of interest, the clusters are thick enough that the semiconductor beneath the clusters makes no contribution. Based on the periodicity and reflection symmetry of the cluster array, this sum was taken in the x-y planes only at the points marked with a cross in Fig. 3(a).

In Fig. 4, such a constructed spectrum, $X(E)$,[23] is compared to an experimental spectrum, $X'(E)$, for the As $3d$ core level taken with 100-eV photon energy. $X(E)$ was constructed for 2 ML of In on 1×10^{19} cm^{-3} p-type GaAs, and the $X'(E)$ is from 1 ML of In on this same doping of p-type GaAs. The experimental spectrum for 3-ML coverage, when normalized, is very similar both in line shape and energy position to the experimental 1-ML spectrum. The spectra $X_0(E)$ and $X'(E)$ were taken with a cylindrical mirror analyzer (CMA) mounted on a stan-

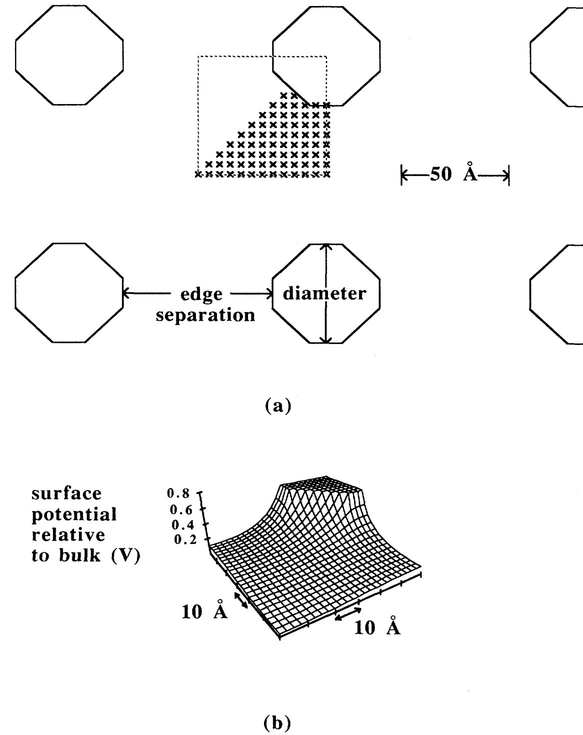

FIG. 3. The parameters in Table I are converted to a periodic array of clusters as an input to STRIDE. (a) View from above of an array representing the 2-ML In coverage. The dashed box encloses the STRIDE input region (Ref. 21). The crosses represent points in the x-y plane from which the STRIDE potential is sampled in order to carry out integral (2). (b) Plot of the surface potential relative to the bulk as calculated by STRIDE for the array of clusters shown in (a) on 1×10^{19} cm^{-3} p-doped GaAs.

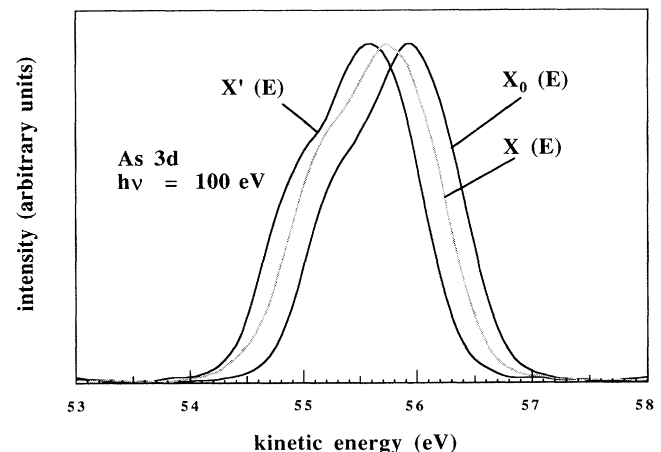

FIG. 4. Plotted here are $X_0(E)$, an As $3d$ spectrum from a cleaved, unpinned p-type GaAs(110) surface; $X(E)$, the "spectrum" constructed for 2-ML In on 1×10^{19} cm^{-3} p-type GaAs; and $X'(E)$, the experimental spectrum for 1-ML In coverage on this doping of GaAs. The peak intensities of the three spectra are normalized to the same value.

dard vacuum chamber at Beamline I-1 of the Stanford Synchrotron Radiation Lab. Further experimental details may be found in Ref. 10. $X_0(E)$, $X(E)$, and $X'(E)$ were curve fit[24] with single bulk and surface components[25] to extract energy shifts and linewidth variations. The calculated band bending for the 2-ML In coverage is 0.16 eV, whereas the measured band bending at 1 (or 3) ML is already 0.4 eV.

For 1×10^{19} cm^{-3} *p*-type GaAs as well as 2×10^{18} and 4×10^{16} cm^{-3} *n*-type GaAs, we repeated this process of (1) taking the cluster geometries from Table I, (2) using STRIDE to compute the potentials around arrays of such clusters, (3) constructing spectra based on these potentials, and (4) curve fitting these spectra to determine energy shifts. Step (4) emulates how experimental spectra are analyzed to determine band bending.

In Fig. 5 the energy shifts of the bulk components are translated into surface Fermi level positions in the GaAs band gap. We noted above that for the 2×10^{18} cm^{-3} *n*-doped GaAs, $\Delta_{\parallel}$ at 0.6-ML coverage is substantially less than the average cluster separation, and Fig. 5 shows that these clusters are calculated to give a band-bending measurement of less than 0.2 eV. On the other hand, the 4×10^{16} cm^{-3} *n*-doped material has roughly ten times larger values of $\Delta_{\parallel}$, and even at the lowest calculated coverage of 0.6 ML, the band bending is near completion. Experimental band-bending data are also plotted in the figure: these In/GaAs data are typical for clustered metal–GaAs interfaces. For the 4×10^{16} cm^{-3} doping there is rough agreement between the calculation and experimental band bending, particularly near the two lowest calculated coverages. For the higher dopings, on the other hand, substantial band bending was measured for In coverages at which the calculated band bending is nearly zero. In fact for the *p*-type GaAs, band bending was first measured at a coverage 3 orders of magnitude lower than that at which the clusters can significantly influence the overall surface potential. So the observation of metallicity in clusters does not necessarily imply that the measured band bending is attributable to this metal.

From Table I and Fig. 2(a), we observe that at coverages above 1 ML, the cluster separations have dropped to a level at which the clusters are expected to deplete the overall surface. As a result the calculated spread among the *n*- and *p*-type surface Fermi levels falls rapidly from 1.3 eV at 0.6-ML coverage to 0.2 eV at 8-ML coverage. Experimentally, however, neither the *n* nor the *p*-type band bending exhibits any sudden increases within this coverage range in which the clusters are calculated to take control of the surface Fermi level: the measured spread is around 0.4 eV throughout this coverage range. Absolute comparisons between, for example, the calculated and experimental *p*-type positions are not possible in this study because the pinning position beneath the In clusters is unknown and not necessarily the value chosen in the model.

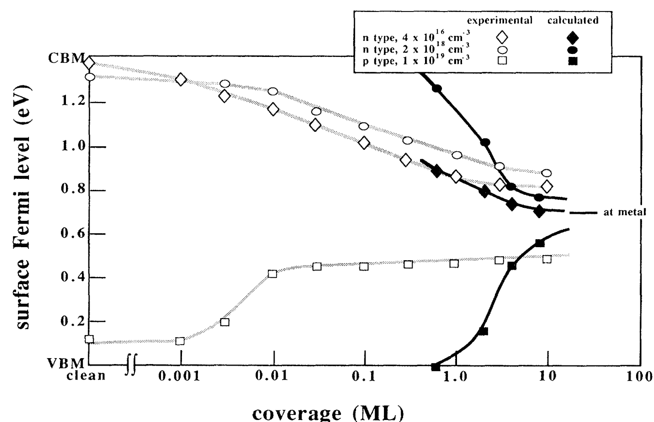

FIG. 5. The calculated surface Fermi level evolution for In on GaAs(110) is compared to the results of PES measurements.

Strong lateral variation in the surface potential should manifest itself as a broadening of the core-level line shapes taken from such surfaces. A slight broadening can be observed in the constructed As 3*d* spectrum of Fig. 3(b). In Table II we list the best fit Gaussian widths obtained in analyzing the constructed spectra. Of course, the broadening produced by integral (2) is not truly Gaussian. The intercluster potentials calculated by STRIDE exhibit broad valleys around the band-bending minima [see Fig. 3(b)]. The value of the potential at these minima dominates integral (2), and thus for *p*-type substrates the broadening is skewed toward higher kinetic energy.

A Gaussian width of 0.43 eV obtains the best fit for the clean cleaved spectrum $X_0(E)$. The widths of the constructed spectra are as much as 25% higher for the intermediate coverages, and they fall off at high coverages when the overall surface potential approaches the value beneath the clusters. On the other hand, for experimental coverages ranging from 0.001 to 10 ML, the best Gaussian fits for the core spectra all fall in the range of 0.42–0.44 eV. Other workers with better instrumental resolution have reported some broadening with overlayer deposition and have partially attributed it to surface-potential inhomogeneity,[26] but certainly no broadening on the scale of Table II was seen in our data. This implies that the surface potential of the experimental interfaces is more uniform than expected from pinning exclusively by the clusters.

The papers by Savage and Lagally[20] are the only systematic measurement of cluster sizes on cleaved III-V semiconductors available in the literature. Thus, only with the In/GaAs(110) system were surface-potential cal-

TABLE II. Best Gaussian widths for $X(E)$, the constructed spectra. The Gaussian width for $X_0(E)$, the unpinned surface spectrum, is 0.43 eV. With the 4×10^{16} cm^{-3} *n*-type GaAs substrate, the best width remains 0.43 eV for all four coverages.

Coverage (ML)	Width for 2×10^{18} cm^{-3} *n*-type GaAs (eV)	Width for 1×10^{19} cm^{-3} *p*-type GaAs (eV)
0.6	0.48	0.51
2	0.47	0.54
4	0.45	0.49
8	0.45	0.48

culations and core-level constructions carried out for various coverages and compared to experiment. However, Svensson, Kanski and Andersson[27] do provide a measurement of cluster sizes on the *(100)* surface of GaAs. These authors studied Ga clusters with SEM for effective coverages of 20, 30, and 50 Å on this surface. For 20-Å coverage they report an average cluster diameter of 235 Å, with a surface coverage of 25%. These measurements translate to an edge separation of roughly 200 Å. Figure 2(a) indicates that for clusters of this size on 2×10^{18} cm^{-3} *n*-doped GaAs, the lateral depletion is about one-quarter of the edge separation, and a strongly varying surface potential is anticipated. An As 3*d* spectrum was constructed for an array of these clusters on this GaAs doping, and the shift of this spectrum was determined to be 0.19 eV. Experimental data for the Ga/GaAs system were taken on the *(110)* surface of 2×10^{18} cm^{-3} *n*-doped GaAs, and for 20-Å coverage the band bending was much higher, nearly 0.8 eV. The Gaussian width of the clean cleaved As 3*d* spectrum is 0.37 eV, and it jumps to 0.46 eV for the constructed spectrum, but the experimental Gaussian width for this same coverage is only 0.39 eV. The cluster morphology on the (110) surface of the PES experiment will differ somewhat from that measured on the (100) surface in Ref. 27, but qualitatively the same strong contrast between constructed and experimental As 3*d* spectra is observed for both In and Ga on GaAs.

For all the clustered systems that have been studied with PES, we can always look at intensity attenuations to estimate cluster sizes. As mentioned above, a lower limit on the cluster separations can be extracted from attenuation data by assuming that the cluster aspect ratios are one. These lower limits verify that the submonolayer band bending observed at these various systems is greater than can be caused by the clusters alone. The lack of substantial broadening in the substrate core-level line shapes from these interfaces provides further confirmation that the surface potential has greater uniformity than is anticipated from the overlayer structure. We conclude that the low coverage band bending at clustered interfaces cannot be attributed to states restricted to the cluster-semiconductor interfaces. Furthermore, the surface Fermi level positions achieved in the low-coverage range often persist at higher coverages, when the clusters should control the surface Fermi level position. In particular an *n*-to-*p* separation of 0.25 eV or more remains to coverages at which the clusters are expected to pin *n*- and *p*-type surfaces at the same position.

V. DISCUSSION

In this section we will consider the implications of the discrepancies between calculation and experiment, illustrated by Fig. 5. But first, we need to review some approximations made in the calculation and show that the discrepancies are not an artifact of these approximations. First of all, experimental factors such as evaporation rate and cleavage quality may lead to some differences in morphology between the samples studied by Savage and Lagally[20] and the samples from which the In/GaAs band bending was measured. But the experimental band bending for the 2×10^{18} and 1×10^{19} cm^{-3} dopings occurs over coverage ranges that are orders of magnitude different than those calculated: such strong qualitative differences cannot be attributed to sample preparation. As mentioned above, PES intensity attenuation provides a lower limit on cluster edge separations that is obtained directly during the band-bending measurements. These edge separation estimates confirm that the clusters cannot be responsible for the low-coverage band bending.

Replacing the regular array of clusters in Fig. 3(a) with a more realistic distribution of clusters is beyond the scope of the present calculation but should primarily result in a broadening of the constructed line shapes, $X(E)$. However, it was observed above in Table II that the line shapes constructed from the ordered cluster array already exhibit greater broadening relative to the clean surface spectrum than is observed in experiment. The effect of disordering the cluster distribution on the energy positions of the constructed spectra would be small at coverages low enough that the clusters are separated by substantially larger distances than the lateral depletion lengths. Furthermore, at coverages high enough that the calculation predicts full depletion of the intercluster surface, a disordering of the distribution will not alter this prediction.

We must further consider that the cluster sizes used in the STRIDE model are average values: the actual interfaces consist of a range of cluster sizes. Taking the average cluster dimensions of Savage and Lagally,[20] Adams, Hitchon, and Holzmann[28] have calculated the range of In cluster sizes on GaAs(110) by simulating the surface diffusion process. They find that the cluster sizes are peaked strongly about the average value, particularly for the 0.6- and 2.0-ML coverages. A secondary peak in the distribution of cluster sizes occurs at the smallest sizes and the influence of such small clusters will be discussed below. Among clusters large enough to be considered metallic, the range of sizes is limited enough that the model of Fig. 3(a) is accurate. Figure 3 of Ref. 28 shows that for a simulated distribution of clusters at 8-ML In coverage, the cluster separations are not substantially different from those of the ordered array.

Thus it is safe to conclude that metal clusters cannot be responsible for the experimental low-coverage band bending at these interfaces, particularly for dopings in the 10^{18}-cm^{-3}range or higher. Thus a source of charge must exist between the clusters to account for the low-coverage band bending observed at the higher dopings. The density of surface states needed to produce such band bending (on the order of 0.7 eV) is only 10^{12} cm^{-2} because these intercluster states are not screened by a metallic overlayer.[12] This density corresponds to less than 0.01 ML.

One possible source of such states goes back to the original suggestion mentioned in the Introduction: a concentration of defects left in the intercluster surface during adatom deposition or cluster condensation.[5] A detailed model has been formulated by Spicer *et al.* for the role of antisite defects in influencing the surface Fermi level position of GaAs.[29] In this model antisites created near the GaAs surface during the interface formation lead to pin-

ning in the neighborhood of defect levels at 0.5 and 0.75 eV above the valence-band maximum.

Another possible source of intercluster surface charge is a submonolayer coverage of adatoms or small nonmetallic clusters between the larger metal clusters. The calculations of Adams, Hitchon, and Holzmann[28] predict such a concentration of small clusters. Of course the exact densities of these clusters depends strongly on the details of the surface diffusion model. Since the density required for substantial band bending is only 0.01 ML, these small clusters would not be detectable in either the substrate PES attenuation or the PES signal from the adatoms themselves. Certainly they would not be detected by RHEED or SEM. Various workers have discussed how individual chemisorbed adatoms or adatom complexes will bend the GaAs bands.[30-32]

A final potential source of surface states is unbuckling of the intercluster surface due to the presence of the metal clusters. Such removal of the reconstruction at the GaAs surface is expected to move donor- and acceptor-type dangling bond states into the GaAs band gap.[33] Interfacial states of this type have been reported in a scanning tunneling microscopy (STM) study of submonolayer Sb coverages on GaAs(110).[34] In this study the states were localized at the periphery of two-dimensional Sb islands. Unless the three-dimensional clusters unbuckle the surface more extensively than this, such unbuckling states, like the clusters themselves, are too inhomogeneously distributed to explain the band-bending measured at low coverages.

We argued above that the high-coverage n-to-p spread observed for these clustered systems is greater than can be attributed to incomplete pinning by the clusters. This spread does not exhibit any significant decrease within the coverage regime in which the clusters are expected to take control of the surface Fermi level. Photovoltaic band flattening can certainly be ruled out as the source of residual spread: for the high-doped substrates at room temperature, this effect is calculated to be zero.[16] Tang and Freeouf[1] have previously discussed the effect of the PES probing depth in separating n- and p-type barrier height measurements. Specifically, the semiconductor potential is sampled for some distance into the substrate, and as a result, the measured potential barrier for both n- and p-type is less than the actual barrier at the surface. This effect has been taken into account in the calculated surface Fermi level positions through the $\int dz\, \exp(-z/\lambda)$ term in Eq. (2), and its influence accounts for part of the small (<0.2 eV) spread seen in the calculated n- and p-type positions of Fig. 5 at 8-ML coverage. This spread also includes some incomplete pinning by the clusters: the calculated n and p positions are still moving closer at 8 ML. The experimental spread is greater than can be accounted for by the combination of the probing depth and incomplete pinning by the clusters.

Thus even when the clusters merge close enough to establish the overall surface Fermi level, the experimental band bending is still an extrapolation of movement observed from submonolayer coverages. This suggests that the intercluster states that caused the initial band bending are now preventing the surface Fermi level from moving to the level at the cluster interface. In other words, the intercluster states may still pin the surface Fermi level even when the clusters are well within a lateral depletion length of one another. We plan to use the Poisson solvers to investigate the influence of donor and acceptor charge states at the intercluster surface. It is of particular interest to determine the density of these states required to pin the surface in the presence of nearby metal clusters.

It is of interest to briefly consider the dependence of the band bending at clustered interfaces on the substrate doping. In Ref. 10, this dependence was investigated for In, Ga, and Ag overlayers on three dopings of n-type GaAs: 4×10^{16}, 5×10^{17}, and 2×10^{18} cm^{-3}. The band bending for In is shown in Fig. 5 for 4×10^{16} and 2×10^{18} cm^{-3} dopings. For all of these overlayers, the band bending is faster on the lower doped substrate, whereas the overlayer morphology is certainly not dependent on the doping. Figure 2(a) of the present paper shows that $\Delta_\parallel$ is always larger for lower doping, and so calculations of the type performed in Sec. IV predict just such a doping dependence. However, it was suggested above that even when $\Delta_\parallel$ becomes larger than the average cluster separation, intercluster states may strongly influence the surface Fermi level position. The band bending $\Delta\phi$ produced by intercluster charges is also anticipated to be faster for a lower doping: for a given surface charge density σ,

$$\Delta\phi=\sigma^2/2\varepsilon_s\varepsilon_0 q N_D \; . \tag{3}$$

The low-coverage band bending in Ref. 10 and Fig. 5 is not as strongly dependent on doping as Eq. (3) indicates. The photovoltaic effect[16] may suppress some of the low-coverage band bending of the lower doped substrates.

For these clustered systems the band bendings for the various n-type dopings merge at coverages for which the n-to-p separation is substantial. For example, in Fig. 5, the n-type band bending is nearly the same (~0.75 eV) for the 4×10^{16} and 2×10^{18} cm^{-3} dopings despite the fact that the n-to-p separation is nearly 0.4 eV. Intercluster midgap states with distinct donor and acceptor levels[5] could account for such behavior. The slightly greater high-coverage barrier height for the lower doped material (in which the range of influence of the metal clusters, $\Delta_\parallel$, is larger) indicates that the states at the cluster-semiconductor interfaces may also have some influence on the surface Fermi level. It is reiterated, however, that the 0.4-eV n-to-p separation cannot be due only to incomplete pinning by the clusters or to the PES probing depth: the influence of such factors on the measured band bending is more strongly doping dependent.[35]

Another work related to the present discussion is the cluster deposition study of Waddill *et al.*[36] These authors deposited "preformed" metal clusters onto GaAs surfaces by initially forming them on a Xe buffer layer and then subliming this buffer. At the highest coverages they examine, the interfaces show less band bending than the normally formed interfaces: 0.3-eV barrier heights for n-type substrates and a distribution of heights concen-

trated around 0.4 eV for *p*-type substrates.[37] Their method of interfacial growth may inhibit the formation of either defects or small adatom clusters between the large metal clusters. These authors observe a distinct step in the band bending between 1- and 10-ML Ag coverage for 2×10^{18} cm^{-3} *p*-doped GaAs, such as was calculated for this range of doping in Fig. 5 for In clusters grown in the absence of intercluster band-bending states.

Having suggested that the band bending measured on clustered systems is controlled by states at the unmetallized surface, one may ask what relevance these measurements have to real Schottky barriers, for which the entire surface is covered. As mentioned previously, separations between *n*- and *p*-type surface Fermi levels on the order of those observed in the PES studies cannot be maintained at the metallized surface.[12] The metal is also expected to influence the energy position and energy distribution of any interfacial gap states.[32,38] Finally the concentrations of these states must be considered and compared to the MIGS density. The band bending observed by PES at the clean surface puts a lower limit on this state density of only 10^{12} cm^{-2}. However, this band bending is substantial at coverages as low as 0.01 ML, and so much higher densities are readily conceivable at the full interface. Tersoff[7] has suggested that the midgap pinning of full metal-semiconductor interfaces can be explained in terms of MIGS alone, but recent calculations based on the method of linear muffin tin orbitals[39] have indicated that intrinsic states at metal-semiconductor interfaces give rise to a greater variation in barrier heights than is observed experimentally. Certainly it would be surprising if the band bending toward midgap observed in the PES measurements is completely unrelated to the midgap pinning determined by electrical measurements at full Schottky barriers.[40]

VI. CONCLUSIONS

In this paper the influence of metal clusters on the surrounding semiconductor surface potential has been quantified. A three-dimensional solution of the Poisson equation shows that the one-dimensional depletion length overestimates the clusters' influence, particularly for small clusters. The surface-potential development was calculated for specific cluster geometries on GaAs, assuming that the pinning states are restricted to the cluster-semiconductor interfaces. We conclude from these calculations that the submonolayer band bending measured by PES from high-doped GaAs is beyond the influence of the clusters and must be attributed to some surface charge states between the clusters. The persistence of a separation between the *n*- and *p*-type surface Fermi level at higher coverages implies that these intercluster states continue to influence the band-bending measurements even when the average cluster separation has shrunk well below the lateral depletion length. To correlate the PES-measured barrier development with that of full metal-semiconductor interfaces, the density of these states relative to MIGS, as well as the influence of the metal on these states, must be considered.

Finally, future experiments are proposed, which may shed further light on the barrier formation at clustered metal-semiconductor interfaces. First, STM images can be taken from such systems to identify sources of surface charge between the clusters. The STM can also measure the potential variation near the edges of the clusters. And as mentioned above, we will be using the Poisson solvers to study the influence of donor and acceptor charge states in the presence of nearby metal clusters.

ACKNOWLEDGMENTS

The authors are grateful to Greg Anderson and Ke-Chih Wu for assistance with the use of PISCES and STRIDE. Two of us (K.E.M. and C.J.S.) were partially supported by IBM. This work was funded by the Defense Advanced Research Projects Agency and by the U.S. Office of Naval Research under Contract No. N00014-89-J-1083.

---

*Present address: IBM Thomas J. Watson Research Center, Yorktown Heights, NY 10598.

[1]J. Y. -F. Tang and J. L. Freeouf, J. Vac. Sci. Technol. B **2**, 459 (1984).

[2]R. Ludeke, T. -C. Chiang, and T. Miller, J. Vac. Sci. Technol. B **1**, 581 (1983).

[3]K. Stiles, A. Kahn, D. G. Kilday, and G. Margaritondo, J. Vac. Sci. Technol. B **5**, 987 (1987); K. Stiles, S. F. Horng, A. Kahn, J. McKinley, D. G. Kilday, and G. Margaritondo, *ibid.* **6**, 1392 (1988).

[4]R. Cao, K. Miyano, T. Kendelewicz, K. K. Chin, I. Lindau, and W. E. Spicer, J. Vac. Sci. Technol B **5**, 998 (1987).

[5]W. E. Spicer, P. W. Chye, P. R. Skeath, C. Y. Su, and I. Lindau, J. Vac. Sci. Technol. **16**, 1422 (1979).

[6]K. Stiles and A. Kahn, Phys. Rev. Lett. **60**, 440 (1988).

[7]J. Tersoff, in *Metallization and Metal-Semiconductor Interfaces,* Vol. 195 of *NATO Advanced Study Institute, Series B: Physics,* edited by I. Batra (Plenum, New York, 1989), p. 281.

[8]J. Tersoff, Phys. Rev. Lett. **52**, 465 (1984), and references cited therein.

[9]Criteria for metallicity have been discussed in W. E. Spicer and R. Cao, Phys. Rev. Lett. **62**, 605 (1989), as well as in Ref. 6. It was usually found that clusters of a hundred or more metal atoms can be treated as bulk metallic.

[10]K. E. Miyano, R. Cao, T. Kendelewicz, C. J. Spindt, P. H. Mahowald, I. Lindau, and W. E. Spicer, J. Vac. Sci. Technol. B **6**, 1403 (1988).

[11]PISCES and STRIDE are semiconductor device modeling programs that can simultaneously solve the Poisson equation and the electron and hole continuity equations over regions of semiconductor, metal, and insulator. In this paper the equilibrium case is of interest, and only the Poisson equation needs to be solved. See M. R. Pinto, C. S. Rafferty, and R. W. Dutton, Stanford University Technical Report, 1984 (unpublished).

[12]A. Zur, T. C. McGill, and D. L. Smith, Phys. Rev. B **28**, 2060 (1983).

[13]PISCES and STRIDE assume that the ionized donors and acceptors provide a constant background of charge. Thus the charge in the depletion region is taken to be uniformly distri-

buted. Even for the highest substrate dopings considered in this study, the ionized donors and acceptors are actually separated by tens of Å. As pointed out in Ref. 1, a more accurate calculation would take the discrete distribution of this charge into account.

[14]PISCES is not necessary for a one-dimensional analysis. Δ_{1D} as established by PISCES is always in excellent agreement with the distance of 90% potential variation that is computed from the simple depletion approximation: $(1-\sqrt{0.1})x_{1D}$, where x_{1D} is expressed in formula (1).

[15]C. M. Aldao, S. G. Anderson, C. Capasso, G. D. Waddill, I. M. Vitomirov, and J. H. Weaver, Phys. Rev. B **39**, 12 977 (1989).

[16]M. H. Hecht, Phys. Rev. B **41**, 7918 (1990).

[17]M. Alonso, R. Cimino, and K. Horn, Phys. Rev. Lett. **64**, 1947 (1990).

[18]R. Cao, K. Miyano, I. Lindau, and W. E. Spicer, J. Vac. Sci. Technol. A **7**, 1975 (1989).

[19]In PES measurements of intensity attenuation, the fraction of the surface covered by the metal f is determined as a function of the effective coverage in Å, θ. For cylindrical clusters with aspect ratio α arranged in a square pattern on the surface, the nearest-neighbor center-to-center separation is $(\sqrt{\pi\theta})/(2\alpha f^{3/2})$. Assuming that θ and f are known, a lower aspect ratio gives a higher cluster separation.

[20]D. E. Savage and M. G. Lagally, J. Vac. Sci. Technol. B **4**, 943 (1986); Phys. Rev. Lett. **55**, 959 (1985).

[21]STRIDE is well suited to such periodic structures because the boundary conditions of the solution region are for zero perpendicular electric field. The infinite array may be solved by limiting the region in the x-y plane to the square bordered by the dashed line in Fig. 3(a).

[22]Many of the III-V semiconductors, GaAs, for example, exhibit flat bands for well-cleaved n- and p-type surfaces. In other words, the surface potential of the cleaved substrate is the same as the potential in the bulk.

[23]From the kinetic-energy range of the experimental spectra, the escape depth λ of Eq. (2) was estimated to be 6 Å. See D. E. Eastman, T. -C. Chiang, P. Heimann, and F. J. Himpsel, Phys. Rev. Lett. **45**, 656 (1980).

[24]For details regarding the curve fitting, see T. Kendelewicz, K. Miyano, R. Cao, J. C. Woicik, I. Lindau, and W. E. Spicer, Surf. Sci. **220**, L726 (1989).

[25]Despite the broadening introduced through integral (2), the constructed $X(E)$ could still be analyzed into surface and bulk components with a surface-to-bulk splitting of about 0.4 eV. The two components were assumed to have the same Gaussian width. The surface-to-bulk intensity ratios did not vary significantly between the fits of $X_0(E)$, $X(E)$, and $X'(E)$.

[26]R. Ludeke and G. Landgren, Phys. Rev. B **33**, 5526 (1986).

[27]S. P. Svensson, J. Kanski, and T. G. Andersson, Phys. Rev. B **30**, 6033 (1984).

[28]J. B. Adams, W. N. G. Hitchon, and L. M. Holzmann, J. Vac. Sci. Technol. A **6**, 2029 (1988).

[29]W. E. Spicer, R. Cao, K. Miyano, T. Kendelewicz, I. Lindau, E. Weber, Z. Liliental-Weber, and N. Newman, Appl. Surf. Sci. **41-42**, 1 (1989).

[30]R. M. Feenstra, J. Vac. Sci. Technol. B **7**, 925 (1989).

[31]W. Mönch, J. Vac. Sci. Technol B **6**, 1270 (1988).

[32]J. E. Klepeis and W. A. Harrison, J. Vac. Sci. Technol. B **7**, (1989).

[33]D. J. Chadi, Phys. Rev. B **18**, 1800 (1978).

[34]R. M. Feenstra and P. Mårtensson, Phys. Rev. Lett. **61**, 447 (1988).

[35]The perpendicular variation of the semiconductor potential at the surface is proportional to $\sqrt{N_D}$ for a simple one-dimensional barrier. Thus the probing depth of the PES should result in a greater band-bending measurement for a lower doped material. This is the same dependence on doping that incomplete pinning by the clusters should manifest.

[36]G. D. Waddill, C. M. Aldao, I. M. Vitomirov, S. G. Anderson, C. Capasso, and J. H. Weaver, J. Vac. Sci. Technol. B **7**, 950 (1989); G. D. Waddill, I. M. Vitomirov, C. M. Aldao, S. G. Anderson, C. Capasso, and J. H. Weaver, Phys. Rev. B **41**, 5293 (1990).

[37]This reduced band bending is probably not due to the photovoltaic band flattening discussed in Ref. 16. The initial sample preparations were performed at 60 K, but the PES measurements were made after warming to desorb the Xe buffer.

[38]R. Ludeke, G. Jezequel, and A. Taleb-Ibrahimi, Phys. Rev. Lett. **61**, 601 (1988).

[39]M. van Schilfgaarde and N. Newman, Phys. Rev. Lett. **65**, 2728 (1990).

[40]The suggestion that the barrier height under the metal may be influenced by defect states or states derived from adatom-substrate bonds is not a contradiction of the original PISCES and STRIDE models for the cluster-semiconductor interfaces. These models assumed that some unspecified source maintains the surface Fermi level of both n- and p-type semiconductors at a certain position in the band gap.